Int. J. Exp. Path. (2006), 87, 227–236
DOI: 10.1111/j.1365-2613.2006.00477.x

ORIGINAL ARTICLE

Developmental abnormalities in multiple proliferative tissues of *Apc*$^{Min/+}$ mice

Shaojin You*, Masami Ohmori*, Maria Marjorette O. Peña†, Basel Nassri*, Jovelyn Quiton*, Ziad A. Al-Assad‡, Lucy Liu*, Patricia A. Wood*, Sondra H. Berger§, ZhiJian Liu§, Michael D. Wyatt§, Robert L. Price¶, Franklin G. Berger** and William J. M. Hrushesky*

**Pathology Core, Center for Colon Cancer Research, Dorn Research Institute, WJB Dorn Veterans Affairs Medical Center (151), Columbia, SC, USA, †Animal Core, Center for Colon Cancer Research, Department of Biological Science, College of Arts and Sciences, University of South Carolina, Columbia, SC, USA, ‡Department of Pathology, WJB Dorn Veterans Affairs Medical Center (151), Columbia, SC, USA, §Department of Basic Pharmaceutical Sciences, College of Pharmacy, University of South Carolina, Columbia, SC, USA, ¶Image Core, Center for Colon Cancer Research, Department of Cell and Developmental Biology & Anatomy, School of Medicine, University of South Carolina, Columbia, SC, USA, and **Director of Center for Colon Cancer Research, Department of Biological Science, College of Arts and Sciences, University of South Carolina, Columbia, SC, USA*

INTERNATIONAL JOURNAL OF EXPERIMENTAL PATHOLOGY

Summary

Germ-line mutation of the *Apc* gene has been linked to familial adenomatous polyposis (FAP) that predisposes to colon cancer. *Apc*$^{Min/+}$ mice, heterozygous for the *Apc* gene mutation, progressively develop small intestinal tumours in a manner that is analogous to that observed in the colon of patients with FAP (Su *et al.* 1992; Fodde *et al.* 1994; Moser *et al.* 1995). We have studied the effects of *Apc* gene mutation on murine intestinal and extra-intestinal, proliferatively active tissues. We have contrasted the histology to that of the age- and sex-matched wild-type C57BL/6 mice. Histological assessment of the normal appearing intestinal mucosa demonstrates minimal change in size of crypts. In contrast, villi are longer in the ileum of *Apc*$^{Min/+}$ mice relative to C57BL/6 mice at 12 and 15 weeks of age. Vigorous splenic haematopoiesis in *Apc*$^{Min/+}$ mice was seen at 12 and 15 weeks of age, as reflected by marked splenomegaly, increased splenic haematopoietic cells and megakaryocytes. Peripheral blood counts, however, did not differ between C57BL/6 and *Apc*$^{Min/+}$ mice at 15 weeks of age. Lymphoid depletion in *Apc*$^{Min/+}$ mice was characterized by diminished numbers of splenic lymphoid follicles and small intestinal Peyer's patches. The ovaries of 12- and 15-week-old *Apc*$^{Min/+}$ mice exhibited increased numbers of atretic follicles, and estrous cycling by serial vaginal smears showed tendency of elongation in the mutant mice during these age ranges. The testicles of 10-week-old *Apc*$^{Min/+}$ mice showed increased numbers of underdeveloped seminiferous tubules. Collectively, these data suggest that, in addition to its obvious effects upon intestinal adenoma formation, *Apc* gene mutation causes impairment of developmental and apparent differentiation blockade in proliferative tissues, including those of the haematopoietic system, lymphoid and reproductive tract.

Received for publication:
17 June 2005
Accepted for publication:
21 October 2005

Correspondence:
William J. M. Hrushesky
Pathology Core
Center for Colon Cancer Research
Dorn Research Institute
WJB Dorn Veterans Affairs Medical Center (151)
6439 Garners Ferry Road
Columbia, SC 29209
USA
Fax: +1 803 6475656;
E-mail: william.hrushesky@med.va.gov

Keywords
gonads, histology, intestine, Min mice, spleen

The $Apc^{Min/+}$ mouse is one of the most commonly used models to investigate the molecular mechanisms of intestinal tumorigenesis. $Apc^{Min/+}$ mice carry a heterozygous germ-line mutation at codon 850 of the *Apc* gene and therefore exhibit haploinsufficiency of APC expression (Su *et al.* 1992). Loss of expression of the normal remaining *Apc* allele in intestinal epithelium necessarily precedes adenoma formation (Luongo *et al.* 1994). At 160-180 days of age, $Apc^{Min/+}$ mice develop approximately 25–75 adenomas in the small intestine and 1–5 in the colon. Concurrently, they become moribund and die with severe anaemia and apparent intestinal obstruction (Moser *et al.* 1990; Su *et al.* 1992). Histology of intestinal polyps or adenomas in $Apc^{Min/+}$ mice has been thoroughly investigated for more than a decade (Moser *et al.* 1990). However, the mechanism by which this precancerous lesion leads to cancer remains unclear. Fewer studies have undertaken histological evaluation of the non-adenomatous intestinal mucosa. For example, Paulsen *et al.* identified two distinct populations of altered crypt foci (ACF_{Min} and classical ACF) in the colon of $Apc^{Min/+}$ mice after azoxymethane (AOM) treatment. The ACF_{Min} were fast growing with altered β-catenin expression and a continuous progression from the monocryptal stage to larger adenomas. In contrast, the classical ACF were slow growing, with normal β-catenin expression, and appeared not to be precancerous (Paulsen *et al.* 2001). Chen *et al.* (2004) investigated gene expression within the normal appearing mucosa that surrounded the intestinal adenomas of $Apc^{Min/+}$ mice and found that several potentially colon cancer-relevant genes (COX-2, CXCR2, MIP-2, Gro-a and OPN) were highly upregulated. They also demonstrated similar gene expression changes in morphologically normal intestinal mucosa taken from surgical sections in human colon cancer patients.

Effects of *Apc* mutation on extra-intestinal organs/tissues have rarely been evaluated. *Apc* gene encodes a large protein (APC) characterized by the presence of several different functional domains that mediate interactions among numerous protein partners (Polakis 1997). APC is postulated to play a role in microtubule dynamics, cell-cycle control, cell adhesion and chromosomal stability (van Es *et al.* 2001). APC is a key component in the WNT-signalling pathway, which is an evolutionarily conserved mechanism that governs cell fate decisions during embryogenesis and in adult tissues. In the mouse, at least 18 different *Wnt* genes have been identified, and several of the genes are expressed in haematopoietic tissues. Recent studies have shown that the WNT-signalling pathway is essential for the regulation of normal haematopoiesis (Reya *et al.* 2000; Yamane *et al.* 2001). Coletta *et al.* have demonstrated that in $Apc^{Min/+}$ mice there is an accelerated and progressive loss of thymocytes beginning at approximately 11 weeks of age with complete regression of the thymus by 17 weeks. In addition, there is profound and parallel depletion of splenic natural killer (NK) cells, and immature B cells, as well as B progenitor cells in bone marrow of $Apc^{Min/+}$ mice. This B-cell depletion is apparently associated with complete loss of interleukin-7 (IL-7)-dependent B-cell progenitors (Coletta *et al.* 2004). Using bone marrow transplantation experiments, Coletta *et al.* further demonstrated that an altered bone marrow microenvironment contributed to these effects (Coletta *et al.* 2004).

To further explore the effects of the *Apc* mutation on tissue proliferation and differentiation, we examined the histology of normal appearing intestinal mucosa and extra-intestinal proliferative organs, including spleen, thymus, testes and ovaries of $Apc^{Min/+}$ mice. We find that the *Apc* gene mutation causes significant histological abnormalities in several proliferative tissues, indicating the importance of the WNT/APC-signalling pathway in the development and differentiation of these tissues.

Materials and methods

Animals

$Apc^{Min/+}$ mice and wild-type C57BL/6 mice were obtained from the Jackson Laboratory (Bar Harbor, ME, USA). Breeding colonies of $Apc^{Min/+}$ and wild-type mice were established in-house, and offsprings were genotyped by using allele-specific polymerase chain reaction (PCR) analysis of tail DNA (Tucker *et al.* 2002). Mice were randomly (on equal health, body weight and sex basis) placed into their respective groups at weaning and provided free access to food and distilled water. Three groups of $Apc^{Min/+}$ mice (8–12/group) at 10, 12 and 15 weeks of age were used in this experiment. Mice were housed four per cage and fed a standard rodent chow (Harlan Teklad Rodent Diet -W, 8604, Harlan Teklad, Madison, WI, USA). Three groups of age-, sex- and diet-

matched C57BL/6 mice housed on an adjacent rack in the same room were used as parallel controls. The Institutional Animal Care and Use Committee of the University of South Carolina approved both the maintenance of animals and experimental protocols.

Daily fertility cycle phase determination and body weight assessment

Additional age-matched female $Apc^{Min/+}$ and C57BL/6 mice (12 mice/group) were studied. The general health condition was monitored by daily assessment of body weight from 12 to 15 weeks of age. Vaginal smears were taken daily using sterile saline, stained with Diff Quick reagent (J.T. Baker, Phillipsburg, NJ, USA), and read by a pathologist using standard criteria (Allen 1922; Bove *et al*. 2002). Daily smears from each mouse were read in sequence to determine the orderly progression of cycling and to classify each smear as proestrus (P), estrus (E), metestrus (M) or diestrus (D). The estrous cycle length (period between the first P of the last cycle to the first P of the next cycle) and cycle frequency (numbers of cycle completed during the vaginal smear period) were compared between the $Apc^{Min/+}$ and C57BL/6 mice.

Autopsy and tissue sample collection & fixation

Mice were euthanized with isoflurane in a vented chemical hood followed by cervical dislocation when they were at 10, 12 and 15 weeks of age. Small intestine, colon, spleen, thymus, testes, blood and ovaries were harvested. Spleen and thymus were weighed. Peripheral blood was collected from mice by retro-orbital eye bleeds, and the white and red blood cell count, haemoglobin concentration and platelet count were determined using an automatic blood cell analyser, VetScanHMT (Abaxis, Union City, CA, USA). Testes were punched with a no. 8 needle and immersed in 10% buffered formalin for 3 h, and cut in half, and then re-immersed in the formalin solution for 24 h. All other organs were fixed by 10% buffered formalin for 24 h and then embedded in paraffin block. Sections were cut at 5-μm thickness, and hematoxylin and eosin-stained (H&E) sections were then prepared for histo-pathological evaluation.

Histological assessment of intestinal tissues

The lumen of intestine (both small intestine and colon) was flushed with Krebs buffer to remove faecal debris and opened using a small scissor longitudinally. The small intestine was equally divided into three segments – the first 1/3 near the stomach (duodenum), the middle 1/3 (jejunum) and the far 1/3 (ileum). The flattened intestinal segments from the four parts of intestinal tissues (duodenum, jejunum, ileum and colon) were rolled into "Swiss rolls", fixed in 10% buffered formalin and embedded in paraffin blocks.

Measurement of villi and crypts

H&E-stained sections were examined with a microscope at ×100 magnification. Three digital images were taken randomly from normal appearing mucosa in each section with a digital camera (AxioCam, Carl Zeiss, Oberkochem Germany). Three straight villi and crypts from each image were measured using the AxioVision software (Carl Zeiss). The length of villus (V) was measured from its tip to its base; the depth of crypt (C) was measured from its opening in the lumen to its base in the lamina propria, and the diameter of neck (ND) was also measured. To minimize the variations from various resources, such as different mouse individuals and sections cut through different longitude axes of villi/cryupts, the size of villus (V) and crypt (C) was compared between two genotypes by the ratios of C/V (CVR), V/ND (VNDR) and C/ND (CNDR).

Peyer's or lymphoid patches are aggregations of lymphatic tissue with clear, delineating boundaries located in the lamina propria of the small intestine and colon, respectively. The number of lymphoid patches in intestinal track was counted using the H&E-stained intestinal sections. The section length of each intestinal segment was measured, and the number of lymphoid follicle was counted in its entirety. The numbers of the lymphoid patches for colon and total numbers of Peyer's patches for small intestines (duodenum, jejunum and ileum) were referenced by the length of the intestinal section (number/cm).

Histological assessments of extra-intestinal tissues

Histology of the selected extra-intestinal tissues (e.g. spleen, thymus, testes and ovaries) were examined microscopically by a pathologist, and digital images were randomly taken by another individual who was not involved in both image and data analysis. The numerical data obtained from images was compared by referencing the area of the tissue section that is being examined.

Spleen. To determine the number of splenic lymphoid follicles (the white pulps), we prepared spleen sections along the longitude axis at the midline. The total area of spleen section (S) was measured, and the number of splenic lymphoid follicles (N) was counted. The density (D) of the follicles was calculated as $D = N/S$ (number/10^6 pixels).

To determine the number of splenic megakaryocytes, we examined the spleen sections microscopically with ×400 magnification (high magnification field, HMF), and five random digital images were taken from red pulp region. The number of megakaryocytes in each image was counted (number/HMF).

To determine the proportion of haematopoietic tissue in red pulp region, we took a microscopic image from the red pulp region of each spleen section at ×100 magnification (low magnification field, LMF). The areas of red pulp and haematopoietic tissue within the red pulp were measured, and the proportion of haematopoietic tissue in the red pulp region was estimated (area of haematopoietic tissue/area of red pulp).

Thymus. The total area of thymus sections (S), the area of cortex (Cox) and the medulla (Med) were measured. The ratios of Cox/S and Med/Cox were calculated and compared across different genotypes of mice.

Testes. Five random digital images were taken at ×100 magnification from each testicular section. The seminiferous tubules were examined to determine whether they were healthy mature (with three continuous layers of spermatocytes – primary, secondary and sperm) or immature or 'under developed' (with fewer or no mature sperm and fewer layers of secondary spermatocytes).

Ovaries. Total area of the ovarian section (S) was measured, and numbers (N) of different stages of ovarian follicles (primary, growing and atretic follicles) were counted. The densities (D) of different stages of ovarian follicles were calculated as follows: D = N/S (number/10^6 pixels).

Statistical analysis

Mean and standard errors were computed to describe average levels of the data. Variance among mean values, across genotypes and/or ages, was contrasted using one- or two-way analysis of variance (ANOVA) or nonparametric analysis, whichever is appropriate, using SAS v8.2 program.

Results

Histological assessment of the small intestine and colon of $Apc^{Min/+}$ mice

As summarized in Table 1, the ratios of VNDR and CNDR decreased with age, and VNDR decreased from the proximal to the distant end of the small intestine in both $Apc^{Min/+}$ and C57BL/6 mice. The VNDR in ileums of $Apc^{Min/+}$ mice at 12 and 15 weeks of age was 21 and 18% higher respectively than those in the age-matched C57BL/6 mice ($P < 0.05$), while the CNDR and CVR in all intestinal segments (duodenum, jejunum, and ileum) at the same age range were equivalent between the $Apc^{Min/+}$ and C57BL/6 mice.

The numbers of Peyer's patches in the small intestine and lymphoid patches in the colon are summarized in Table 2. The average number of Peyer's patches in the small intestine of 15-week-old $Apc^{Min/+}$ mice was significantly lower compared with that in the wild-type C57BL/6 mice ($P = 0.012$).

Histological assessment of spleen

The spleen is a major extramedullary haematopoietic and immune organ in rodents. The spleen weight of $Apc^{Min/+}$ mice increased 2.7-fold from 10 to 15 weeks of age (i.e. from 81 to 217 mg). On the other hand, the spleens of C57BL/6 mice did not exhibit this weight increase (Table 3).

Histological analysis revealed that both the mass and cellularity of the red pulp in spleens of 15-week-old $Apc^{Min/+}$ mice were significantly higher than those of the age-matched C57BL/6 mice (Figure 1a,c). The red pulp region contains haematopoietic progenitors and differentiated cells, such as megakaryocytes and erythroblasts/megaloblasts. In the red pulp of spleens from wild-type mice, these haematopoietic progenitor cells were rare (Figure 1a,b). In contrast, in $Apc^{Min/+}$ mice, most spleens exhibited increased numbers and clusters of megakaryocytes, erythroblast- or megaloblast-like cells (Figure 1d,e). The proportion of haematopoietic cells in the red pulp of $Apc^{Min/+}$ mice was approximately twofold higher than that in red pulp of spleens of the age-matched C57BL/6 mice (Figure 1f) ($P < 0.05$). Megakaryocytes, which often proliferate during splenic haemotapoiesis, are giant cells and easily identified. Megakaryocytes were scattered or formed small clusters in spleens of both $Apc^{Min/+}$ and C57BL/6 mice (Figure 1d). The numbers of these cells were significantly higher in the red pulp of 15-week-old $Apc^{Min/+}$ mice as compared with the age-matched C57BL/6 mice (9.4 *vs.* 5.3, $P < 0.05$, Table 3).

The size and morphology of splenic lymphoid follicles comprising the white pulp appear normal in $Apc^{Min/+}$ mice with no genotype differences observed, when compared with that of C57BL/6 mice. The number of lymphoid

Table 1 Genotype and age differences in small intestinal villi and crypt measurements

	VNDR		CNDR		CVR	
Mice	**12 week**	**15 week**	**12 week**	**15 week**	**12 week**	**15 week**
Duodenum						
$Apc^{Min/+}$	17.45 ± 0.98	14.09 ± 0.60	4.30 ± 0.30	3.21 ± 0.14	0.24 ± 0.01	0.24 ± 0.01
C57BL/6	17.33 ± 0.94	14.27 ± 0.43	4.72 ± 0.28	3.39 ± 0.18	0.24 ± 0.01	0.23 ± 0.02
Jejunum						
$Apc^{Min/+}$	10.49 ± 1.34	8.73 ± 0.39	5.06 ± 0.54	3.69 ± 0.13	0.40 ± 0.02	0.41 ± 0.03
C57BL/6	10.37 ± 1.19	9.18 ± 0.37	5.39 ± 0.32	3.68 ± 0.18	0.41 ± 0.04	0.43 ± 0.03
Ileum						
$Apc^{Min/+}$	7.57 ± 0.59*	7.43 ± 0.27†	4.87 ± 0.37	4.42 ± 0.15	0.64 ± 0.05	0.65 ± 0.03
C57BL/6	6.24 ± 0.52*	6.28 ± 0.43†	4.48 ± 0.26	3.97 ± 0.17	0.58 ± 0.02	0.60 ± 0.02

CNDR, crypt depth/neck diameter of crypt; CVR, ratio of crypt depth/villi length; VNDR, ratio of villi length/neck diameter of crypt.
*, Significant genotype difference, $P < 0.05$.

Table 2 Genotype differences in number of Peyer's (small intestine) and lymphoid patches (colon) in the intestinal tract

	Small intestine (number/cm)			Colon (number/cm)		
Mouse group	**10 week**	**12 week**	**15 week**	**10 week**	**12 week**	**15 week**
$Apc^{Min/+}$	1.18 ± 0.12	1.13 ± 0.27	1.03 ± 0.14*	2.12 ± 0.86	1.67 ± 0.57	2.21 ± 0.27
C57BL/6	1.30 ± 0.22	1.25 ± 0.21	1.66 ± 0.18*	2.88 ± 0.62	1.76 ± 0.41	2.66 ± 0.49

*Genotype differences, $P = 0.012$.

follicles, which reached a maximum at 12 weeks of age in both $Apc^{Min/+}$ and C57BL/6 mice, decreased significantly by 15 weeks of age in $Apc^{Min/+}$ mice (i.e. from 178.3/10^6 pixels to 87.23/10^6 pixels). In contrast, the decrease in splenic lymphoid follicles in C57BL/6 mice of the same age was much less (i.e. from 200.5/10^6 pixels to 148.92/10^6 pixels). Thus, by 15 weeks of age, there were significantly fewer splenic lymphoid follicles in $Apc^{Min/+}$ mice compared with the age-matched C57BL/6 mice ($P < 0.05$, Table 3).

Table 3 Histological differences of splenic weight, splenic lympoid follicles and splenic megakaryocytes between $Apc^{Min/+}$ and C57BL/6 mice

	Age groups		
Mouse	**10 week**	**12 week**	**15 week**
Weight (mg)			
$Apc^{Min/+}$	82.6 ± 3.4	120.0 ± 9.6*	216.7 ± 52.1†
C57BL/6	76.9 ± 5.8	82.1 ± 6.8*	86.4 ± 3.5†
Lymph. follicle (number/10^6 pixel)			
$Apc^{Min/+}$	81.0 ± 6.0	172.3 ± 23.3	87.2 ± 18.8‡
C57BL/6	92.7 ± 7.1	200.5 ± 16.6	145.3 ± 10.4‡
Megakaryocytes(number/HMF)			
$Apc^{Min/+}$	3.6 ± 0.5	3.8 ± 0.5	9.4 ± 1.5§
C57BL/6	4.0 ± 0.9	3.8 ± 0.5	5.3 ± 0.6§

*, †, ‡, §, Genotype differences, $P < 0.05$.

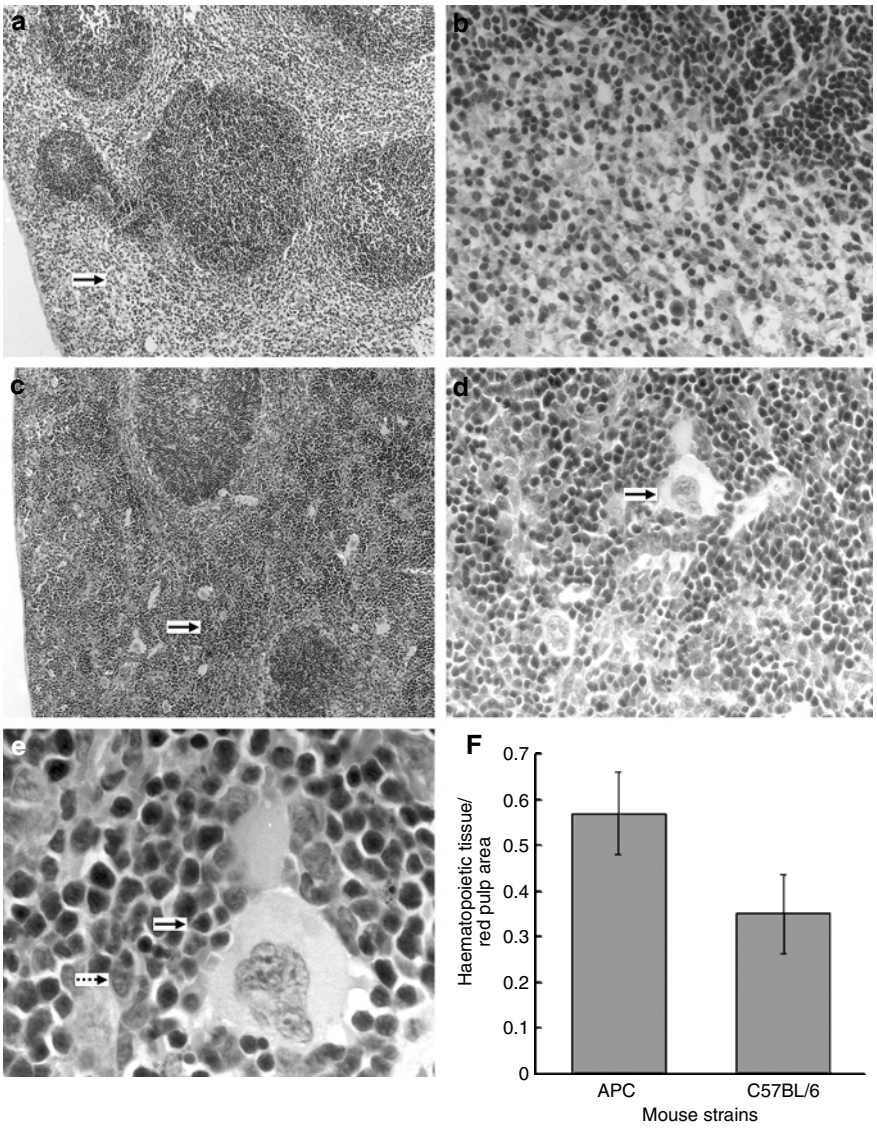

Figure 1 Photomicrograph of spleens from wild type C57BL/6 (**a,b**) and $Apc^{Min/+}$ (**c,d,e**) mice. The red pulp of the wild type spleens ((**a**) bold arrow) is characterized by a loose, reticular mesh structure with small, mature lymphocytes, no splenic megaloblasts, only a few megakaryocytes, and large blood-filled sinuses ((**a**) magnification ×10 (**b**) ×40). The spleen red pulp of $Apc^{Min/+}$ mice show increased cellularity ((**c**) ×10, bold arrow), increased clusters of splenic megakaryocytes ((**d**) ×40, bold arrow), increased erythroblasts ((**e**) ×100, bold arrow) and increased megaloblasts ((**e**) dotted arrow). The proportion of splenic hematopoietic tissue in $Apc^{Min/+}$ mice (**f**) was significantly higher than that in the wild type mice ($P=0.018$).

Thymus

It has been reported that thymic atrophy occurs in $Apc^{Min/+}$ mice beginning at about 80 days of age with cortical thinning becoming obvious by 100 days (Coletta *et al.* 2004). We did not find significant thymic atrophy in the $Apc^{Min/+}$ mice, as evaluated by weight of the organ, cortical thickness or the ratio of medulla/cortex (Table 4). Thymocytes were abundant

Table 4 Genotype comparisons in the weight, ratio of cortex/total and medulla/cortex of thymus

Age	Mice	Thymus wt (mg)	Cortex/total (%)	Medulla/cortex (%)
10 week	$Apc^{Min/+}$	67.5 ± 3.3	71.4 ± 2.0	41.0 ± 3.9
	C57BL/6	58.4 ± 2.9	72.6 ± 2.0	38.5 ± 3.8
15 week	$Apc^{Min/+}$	57.6 ± 5.0	71.5 ± 2.5	41.1 ± 5.4
	C57BL/6	68.6 ± 6.4	73.3 ± 1.7	37.2 ± 3.4

No statistical differences were found.

Table 5 Genotype differences in histology of reproductive tissues

Mouse group	Seminiferous tubules (number/LMF)		Ovarian follicles (number/10^6 pixel)		
	Healthy	Underdeveloped	Primary + Growing	Mature	Atretic
10 week					
$Apc^{Min/+}$	30.3 ± 3.8	4.25 ± 1.5*	49.4 ± 7.9	2.1 ± 0.7	15.3 ± 1.2†
C57BL/6	34.0 ± 1.5	0.25 ± 0.3*	37.5 ± 7.5	1.6 ± 0.5	10.2 ± 2.5†
12 week					
$Apc^{Min/+}$	37.0 ± 3.8	2.25 ± 0.8	52.7 ± 7.2	5.1 ± 1.9	47.3 ± 16.1‡
C57BL/6	36.3 ± 4.1	1.5 ± 0.9	74.6 ± 10.7	2.0 ± 0.2	12.3 ± 0.9‡
15 week					
$Apc^{Min/+}$	52.0 ± 5.8	1.75 ± 0.6	79.9 ± 29.6	7.1 ± 1.4	37.4 ± 11.6
C57BL/6	55.2 ± 4.6	2.00 ± 1.1	38.4 ± 8.5	4.2 ± 1.9	26.9 ± 1.9

Genotype difference, *$P = 0.03$, †$P = 0.07$, ‡$P = 0.049$.

in the cortex in both mutant and wild-type mice with no major differences.

Reproductive tissues

Most seminiferous tubules in the testes of $Apc^{Min/+}$ mice appeared normal. There were more underdeveloped seminiferous tubules in the testes of the 10-week-old $Apc^{Min/+}$ mice than their C57BL/6 counterparts (Table 5). These tubules were recognized by decreased layers of spermatocytes (especially secondary spermatocytes) and loss of mature spermatozoa in the lumen.

In the ovaries, various stages of ovarian follicles (primary, growing, mature and atretic follicles) and corpora lutea were present in $Apc^{Min/+}$ mice (Figure 2a,b). The numbers of primary and growing follicles were about twofold higher in $Apc^{Min/+}$ mice relative to C57BL/6 mice at 15 weeks of age, although this difference was not statistically significant ($P > 0.05$). However, the numbers of atretic follicles in each of the three age groups of $Apc^{Min/+}$ mice were higher than in C57BL/6 mice, with the difference being statistically significant in 12-week-old mice (Table 5). The numbers of atretic follicles in ovaries of three of seven (43%) $Apc^{Min/+}$ mice at 12 and 15 weeks of age were more than threefold higher than the average number of atretic ovarian follicle in C57BL/6 mice.

From 12 to 15 weeks of age, body weights of the $Apc^{Min/+}$ mice increased gradually from 19.35 ± 0.36 to 22.52 ± 0.64 g, while a similar increase was seen in that of C57BL/6 mice (from 19.95 ± 0.21 to 23.1 ± 0.38 g). There was no major health problem observed in the $Apc^{Min/+}$ mice at the end of this experimental period. Vaginal cytologies showed no obvious qualitative changes in daily vaginal smears of $Apc^{Min/+}$ and C57BL/6 mice. The $Apc^{Min/+}$ mice completed the same number of estrous cycles as did C57BL/6 mice (2.55 ± 0.21 *vs.* 2.44 ± 0.24, $P = 0.82$) in a fixed number of days, although the length of estrous cycle of $Apc^{Min/+}$ mice was slightly longer than in C57BL/6 mice (5.20 ± 0.77 *vs.* 3.88 ± 0.93, $P = 0.06$).

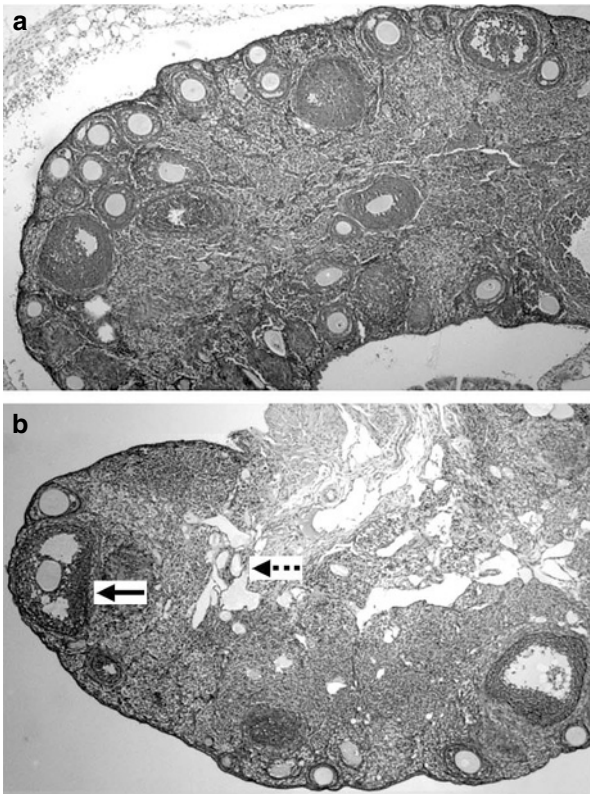

Figure 2. Photomicrograph of ovaries from wild type C57BL/6 and $Apc^{Min/+}$ mice (magnification ×10). (**a**) The ovaries from wild type mice are normal, characterized by follicles in various stages of development. (**b**) Ovaries from $Apc^{Min/+}$ type show normal primary growing and mature follicles (bold arrow). However, the number of the atretic follicles in the central region of the ovary is significant increased (dotted arrow).

Table 6 Blood counts of $Apc^{Min/+}$ and C57BL/6 mice at 15-week old

Mice	WBC ($\times 10^3$/ml)	Lym ($\times 10^3$/ml)	Mon ($\times 10^3$/ml)	Gra ($\times 10^3$/ml)	RBC ($\times 10^6$/ml)	Hb (g/dl)	PLT ($\times 10^9$/l)
$Apc^{Min/+}$	10.35 ± 0.62	7.58 ± 0.84	0.34 ± 0.03	2.43 ± 0.32	7.14 ± 0.21	15.56 ± 0.52	341.29 ± 23.38
C57BL/6	10.80 ± 0.57	8.60 ± 0.40	0.33 ± 0.02	1.87 ± 0.16	6.99 ± 0.09	15.23 ± 0.19	325.22 ± 18.33

No statistical differences were found. Normal ranges of Hb in mouse: 12.2 – 16.2 (g/dl) (Sirois 2002).

Blood cell counts

Table 6 summarizes the results of complete blood cell counts and white blood cell differential counts from both the mutant and wild-type mice at 15 weeks of age. There were no significant differences in blood cell counts at this age.

Discussion

The $Apc^{Min/+}$ mouse model is frequently used to study the effects of the interaction of genetics, diet or chemical compounds on the development of intestinal neoplasia. The genetic predisposition for intestinal neoplasia becomes obvious in $Apc^{Min/+}$ mice by 3 weeks of age, with tumours being initiated through loss of expression of the wild-type *Apc* allele (Kettunen *et al.* 2003). Chen *et al.* (2004) have shown that the normal mucosa from $Apc^{Min/+}$ mice or from human colon cancer patients show many changes in gene expression relative to wild-type mice or normal control subjects. These data imply that morphologically normal colonic mucosa in $Apc^{Min/+}$ mice and in colon cancer patients is altered. Intestinal epithelium of $Apc^{Min/+}$ mice carries a mutation in one allele of the *Apc* gene; thus, any area of intestinal mucosa may, presumably, develop polyps. The general histology of the non-adenomatous mucosa, however, has not been fully described. Kettunen *et al.* (2003) reported that the villus/crypt ratio (CVR) in the ileum is not different between the wild-type and *Apc*-mutant mice. We further demonstrate that the CVRs in all small intestinal segments from both genotypes are similar. In an evaluation of the data of villous length and crypt depth, we have noticed significant variations in the measurements from various resources, such as variation between individual mice and variations as to whether the sections were cut through different axes of villi or crypts. Among those, the latter case generates greater variations. For example, the lengths of villi are different when sections are cut longitudinally through the midline or side axes of the villi. This variation can be minimized if the length of the villus is referenced to the diameter of the crypt neck (ND), because the neck is cut simultaneously with the villus. In addition, the ND is rarely affected or affected to a much less extent by stimuli of inflammation and/or cell proliferation, and thus VNDR is a reliable measurement to evaluate the length of the villi. As summarized in Table 1, significant differences were found in the length of villi in the ileum of both 12- and 15-week-old $Apc^{Min/+}$ mice, as compared with the age-matched wild-type C57BL/6 mice. It is not known how the elongation of ileal villi relates to the process of tumorigenesis in these mice. In human and rodent intestines, APC expression is restricted to the luminal half of the crypt, a nonproliferative, differentiated zone (Smith *et al.* 1993), because cells move up from the crypt and then are normally shed into the lumen from this region following apoptosis. The elongation of the ileal villi may imply a decrease in apoptosis, leading to an elongation in villi length and to a predilection to adenoma formation.

Most of the adenomas start to appear in $Apc^{Min/+}$ mice at 5–8 weeks of age, and no significant increase in the number of adenomas is observed thereafter (Kettunen *et al.* 2003). Puberty begins around the fifth week of life in most inbred mouse strains such as C57BL/6 (Nelson *et al.* 1990; Joshi *et al.* 1995). At puberty, T cells differentiate in thymus and migrate into peripheral tissues, and the numbers of $CD8^+$ and Mac-1^+ cells and the intestine-luminal concentrations of IgA and PGE_2 increase significantly (Guevara Patino *et al.* 2000). It seems likely that the rise of sex hormones associated with puberty terminates the initial process of adenomagenesis in the intestinal epithelium, either through immunologic or other, more direct, means (Kettunen *et al.* 2003). The relevance of the pubertal events to the development of adenomas is also strongly supported by the clinical knowledge that the polyps of familial adenomatous polyposis (FAP) patients are seldom seen before 10 years of age (Ruttenberg *et al.* 1991). We found that the numbers of splenic lymphoid follicles and intestinal (small intestine) lymphoid patches were significantly diminished in $Apc^{Min/+}$ mice at 15 weeks of age but not earlier. Because this lymphoid depletion appears weeks after the initial appearance of intestinal polyps, it is unlikely to be its sole cause.

Coletta *et al.* (2004) have reported that the thymus and lymph nodes of $Apc^{Min/+}$ mice regress progressively, and

both immature and mature T and B lymphocytes are lost beginning at about 12 weeks of age. We have confirmed that the lymph follicles in both spleen and small intestine of $Apc^{Min/+}$ mice are significantly depleted by 15 weeks of age. However, we did not observe thymic atrophy in $Apc^{Min/+}$ mice, at either 10 or 15 weeks of ages. The reason for the discrepancy remains unknown, although our thymic endpoints are more general (e.g. weight and area).

The importance of the spleen in murine haematopoiesis has been demonstrated in a number of stress states, such as cytokine exposure, cytotoxic exposure and virus infection (Morse *et al.* 1978; Yeager *et al.* 1983; Patchen *et al.* 1994; Slayton *et al.* 2002). Increased splenic megakaryopoiesis has been observed in response to various pharmacological agents (Yeager *et al.* 1983; Shiotsu *et al.* 1998), as well as in leukemic (Ritchie *et al.* 1999) and myeloproliferative states (Slayton *et al.* 2002). We have observed significantly increased splenic megaloblasts and megakaryopoiesis in $Apc^{Min/+}$ mice at 15 weeks of age, despite normal peripheral blood cell counts. Such enhancement of haematopoiesis may be due to a compensatory response to blood loss associated with chronic bleeding from necrotic intestinal polyps. However, this explanation is inconsistent with the fact that the 15-week-old $Apc^{Min/+}$ mice were not anaemic at sacrifice. Enhanced splenic haematopoiesis, therefore, must be a consequence of some other physiological event(s). The *Apc* gene product plays a pivotal role in the WNT-signalling pathway. Downregulation of APC results in the accumulation of β-catenin, a primary end product of the pathway that maintains the proliferative state of cells (Kongkanuntn *et al.* 1999; Fodde 2002). Proper cell differentiation requires repression of β-catenin. We propose that *Apc* gene mutation-associated β-catenin overproduction associated with the *Apc* gene mutation impedes the normal development and differentiation in a wide range of tissues. This is particularly relevant to haematopoietic tissues, where stem cells and progenitors with impaired potential to fully differentiate fail to mature, resulting in lymphoid depletion and extramedullary haematopoiesis (Liu *et al.* 2005). While this initially occurs in absence of anemia, it can eventually become so severe as to result in anaemia at later ages (Moser *et al.* 1990; Su *et al.* 1992).

Additional evidence that *Apc* mutation impairs the differentiation of stem cells comes from histological observations of other tissues. Moser *et al.* (1993) have found that the mammary gland of $Apc^{Min/+}$ mice is predisposed to premalignant alveolar hyperplasia. In the testes, at 10 weeks after puberty, we found more morphologically underdeveloped seminiferous tubules in $Apc^{Min/+}$ mice than in C57BL/6 mice. This early pathological abnormality did not, however, progress with advancing age, because the numbers of underdeveloped tubules were largely equal later in life between the $Apc^{Min/+}$ and C57BL/6 mice. Bennett *et al.* (2001) have described mild testicular degeneration in approximately 11% (1/9) of both $Apc^{Min/+}$ and wild-type mice at 100 days of age. In the ovary, we found a greater than threefold increase in the number of atretic follicles in three of seven (43%) of the 12- and 15-week-old $Apc^{Min/+}$ mice, indicating that many ovarian follicles develop but fail to fully mature in these mice, which may impair sex hormone production and reproductive function. Vaginal cytologies showed tendency of estrous cycle elongation in $Apc^{Min/+}$ mice during the observed period (from 12 to 15 weeks of age). Bennett *et al.* reported the absence of corpora lutea and/or complete follicular atrophy in the ovaries of approximately one-fourth of $Apc^{Min/+}$ mice at 100 days of age. This premature ovarian failure may have secondary effects upon other female reproductive tissues. For example, the uterine endometrium and myometrium appear quiescent, reminiscent of an immature appearance. In addition, the vaginal epithelium is reduced in thickness and lined by vacuolated cells (Bennett *et al.* 2001). Premature failure of ovarian follicles affects the reproductive function of $Apc^{Min/+}$ mice and may contribute, in part, the reduced fertility and fecundity in these animals (Moser *et al.* 1990).

In summary, the qualitative and quantitative histological survey of the haematopoietic, reproductive and intestinal epithelial tissues in $Apc^{Min/+}$ mice reveals abnormalities that are consistent with impairment of normal tissue differentiation. This is likely due to constitutive overproduction of β-catenin caused by *Apc* gene mutation. These findings indicate the $Apc^{Min/+}$ model to be useful in the study of the role of the WNT-signalling pathway in tissue differentiation and organ development.

Acknowledgements

We thank Yin Xiong, Mei Li, John Murphy, Celestia Davis and Jody Tucker for their kind assistance of tissue and blood sample harvesting and processing. This work is supported by NIH/NCRR (COBRE) grant P20RR17698-01.

References

Allen E. (1922) The oestrous cycle in the mouse. *Am. J. Anat.* **30**, 297–348.

Bennett L.M., McAllister K.A., Ward T. *et al.* (2001) Mammary tumor induction and premature ovarian failure in ApcMin mice are not enhanced by Brca2 deficiency. *Toxicol. Pathol.* **29**, 117–125.

Bove K., Lincoln D.W., Wood P.A., Hrushesky W.J. (2002) Fertility cycle influence on surgical breast cancer cure. *Breast Cancer Res. Treat.* **75**, 65–72.

Chen L.C., Hao C.Y., Chiu Y.S. *et al.* (2004) Alteration of gene expression in normal-appearing colon mucosa of APC (min) mice and human cancer patients. *Cancer Res.* **64**, 3694–3700.

Coletta P.L., Muller A.M., Jones E.A. *et al.* (2004) Lymphodepletion in the ApcMin/+ mouse model of intestinal tumorigenesis. *Blood* **103**, 1050–1058.

van Es J.H., Giles R.H., Clevers H.C. (2001) The many faces of the tumor suppressor gene APC. *Exp Cell Res.* **264**, 126–134.

Fodde R. (2002) The APC gene in colorectal cancer. *Eur J. Cancer* **38**, 867–871.

Fodde R., Edelmann W., Yang K. *et al.* (1994) A targeted chain-termination mutation in the mouse Apc gene results in multiple intestinal tumors. *Proc. Natl. Acad. Sci. USA* **91**, 8969–8973.

Guevara Patino J.A., Marino M.W., Ivanov V.N., Nikolich-Zugich J. (2000) Sex steroids induce apoptosis of CD8+CD4+ double-positive thymocytes via TNF-alpha. *Eur J. Immunol.* **30**, 2586–2592.

Joshi D., Billiar R.B., Miller M.M. (1995) Luteinizing hormone response to N-methyl-D, L-aspartic acid in the presence of physiological estradiol concentrations: influence of age and the ovary. *Proc. Soc. Exp. Biol. Med.* **209**, 237–244.

Kettunen H.L., Kettunen A.S., Rautonen N.E. (2003) Intestinal immune responses in wild-type and ApcMin/+ mouse, a model for colon cancer. *Cancer Res.* **63**, 5136–5142.

Kongkanuntn R., Bubb V.J., Sansom O.J., Wyllie A.H., Harrison D.J., Clarke A.R. (1999) Dysregulated expression of beta-catenin marks early neoplastic change in Apc mutant mice, but not all lesions arising in Msh2 deficient mice. *Oncogene* **18**, 7219–7225.

Liu Z.J., Yon S., Hrushesky W.J.M., *et al.* (2005) Possible role of APC gene in hematopoiesis: An implication for anemia $Apc^{min/+}$ mice. *Proc Am Assoc Cancer Res* **46**, 1980.

Luongo C., Moser A.R., Gledhill S., Dove W.F. (1994) Loss of Apc+ in intestinal adenomas from Min mice. *Cancer Res.* **54**, 5947–5952.

Morse B., Giuliani D., Fredrickson T., LoBue J. (1978) Erythrokinetics and ferrokinetics of a viral-induced murine erythroblastosis. *Blood* **51**, 623–632.

Moser A.R., Luongo C., Gould K.A., McNeley M.K., Shoemaker A.R., Dove W.F. (1995) ApcMin: a mouse model for intestinal and mammary tumorigenesis. *Eur J. Cancer* **31A**, 1061–1064.

Moser A.R., Mattes E.M., Dove W.F., Lindstrom M.J., Haag J.D., Gould M.N. (1993) ApcMin, a mutation in the murine Apc gene, predisposes to mammary carcinomas and focal alveolar hyperplasias. *Proc. Natl. Acad. Sci. USA* **90**, 8977–8981.

Moser A.R., Pitot H.C., Dove W.F. (1990) A dominant mutation that predisposes to multiple intestinal neoplasia in the mouse. *Science* **247**, 322–324.

Nelson J.F., Karelus K., Felicio L.S., Johnson T.E. (1990) Genetic influences on the timing of puberty in mice. *Biol. Reprod.* **42**, 649–655.

Patchen M.L., Fischer R., Schmauder-Chock E.A., Williams D.E. (1994) Mast cell growth factor enhances multilineage hematopoietic recovery in vivo following radiation-induced aplasia. *Exp. Hematol.* **22**, 31–39.

Paulsen J.E., Steffensen I.L., Loberg E.M., Husoy T., Namork E., Alexander J. (2001) Qualitative and quantitative relationship between dysplastic aberrant crypt foci and tumorigenesis in the Min/+ mouse colon. *Cancer Res.* **61**, 5010–5015.

Polakis P. (1997) The adenomatous polyposis coli (APC) tumor suppressor. *Biochim. Biophys. Acta.* **1332**, F127–F147.

Reya T., O'Riordan M., Okamura R. *et al.* (2000) Wnt signaling regulates B lymphocyte proliferation through a LEF-1 dependent mechanism. *Immunity* **13**, 15–24.

Ritchie K.A., Aprikyan A.A., Bowen-Pope D.F. *et al.* (1999) The Tel. PDGFRbeta fusion gene produces a chronic myeloproliferative syndrome in transgenic mice. *Leukemia* **13**, 1790–1803.

Ruttenberg D., Elliot M.S., Bolding E. (1991) Severe colonic dysplasia in a child with familial adenomatous polyposis. *Int. J. Colorectal Dis.* **6**, 169–170.

Shiotsu Y., Akinaga S., Yamashita K. *et al.* (1998) In vitro and in vivo effects of KT6352, a derivative of indolocarbazole compounds, on murine megakaryocytopoiesis. *Exp Hematol.* **26**, 1195–1201.

Sirois M. (2002) *Laboratory Animal Medicine*, 2nd edn. American College of Laboratory Animal Medicine Series, Academic Press, Mosby Inc. (St Louis, MO, USA)

Slayton W.B., Georgelas A., Pierce L.J. *et al.* (2002) The spleen is a major site of megakaryopoiesis following transplantation of murine hematopoietic stem cells. *Blood* **100**, 3975–3982.

Smith K.J., Johnson K.A., Bryan T.M. *et al.* (1993) The APC gene product in normal and tumor cells. *Proc. Natl. Acad. Sci. USA* **90**, 2846–2850.

Su L.K., Kinzler K.W., Vogelstein B. *et al.* (1992) Multiple intestinal neoplasia caused by a mutation in the murine homolog of the APC gene. *Science* **256**, 668–670.

Tucker J.M., Davis C., Kitchens M.E. *et al.* (2002) Response to 5-fluorouracil chemotherapy is modified by dietary folic acid deficiency in Apc (Min/+) mice. *Cancer Lett.* **187**, 153–162.

Yamane T., Kunisada T., Tsukamoto H. *et al.* (2001) Wnt signaling regulates hemopoiesis through stromal cells. *J. Immunol.* **167**, 765–772.

Yeager A.M., Levin J., Levin F.C. (1983) The effects of 5-fluorouracil on hematopoiesis: studies of murine megakaryocyte-CFC, granulocyte-macrophage-CFC, and peripheral blood cell levels. *Exp. Hematol.* **11**, 944–952.